BIOCHEMISTRY
including biophysical chemistry & molecular biology

ARTICLE

pubs.acs.org/biochemistry

The Intracellular Distal Tail of the Na^+/H^+ Exchanger NHE1 Is Intrinsically Disordered: Implications for NHE1 Trafficking

Ann-Beth Nørholm,[†,‡] Ruth Hendus-Altenburger,[†,‡] Gabriel Bjerre,[†] Magnus Kjaergaard,[‡] Stine F. Pedersen,[*,†] and Birthe B. Kragelund[*,‡]

[†]Cell and Developmental Biology, Department of Biology, University of Copenhagen, Universitetsparken 13, DK-2100 Copenhagen Ø, Denmark

[‡]Structural Biology and NMR Laboratory, Department of Biology, University of Copenhagen, Ole Maaløes Vej 5, DK-2200 Copenhagen N, Denmark

Supporting Information

ABSTRACT: Intrinsic disorder is important for protein regulation, yet its role in regulation of ion transport proteins is essentially uninvestigated. The ubiquitous plasma membrane carrier protein Na^+/H^+ Exchanger isoform 1 (NHE1) plays pivotal roles in cellular pH and volume homeostasis, and its dysfunction is implicated in several clinically important diseases. This study shows, for the first time for any carrier protein, that the distal part of the C-terminal intracellular tail (the *cdt*, residues V686−Q815) from human (h) NHE1 is intrinsically disordered. Further, we experimentally demonstrated the presence of a similar region of intrinsic disorder (ID) in NHE1 from the teleost fish *Pleuronectes americanus* (paNHE1), and bioinformatic analysis suggested ID to be conserved in the NHE1 family. The sequential variation in structure propensity as determined by NMR, but not the amplitude, was largely conserved between the h- and paNHE1*cdt*. This suggests that both proteins contain molecular recognition features (MoRFs), i.e., local, transiently formed structures within an ID region. The functional relevance of the most conserved MoRF was investigated by introducing a point mutation that significantly disrupted the putative binding feature. When this mutant NHE1 was expressed in full length NHE1 in AP1 cells, it exhibited impaired trafficking to the plasma membrane. This study demonstrated that the distal regulatory domain of NHE1 is intrinsically disordered yet contains conserved regions of transient structure. We suggest that normal NHE1 function depends on a protein recognition element within the ID region that may be linked to NHE1 trafficking via an acidic ER export motif.

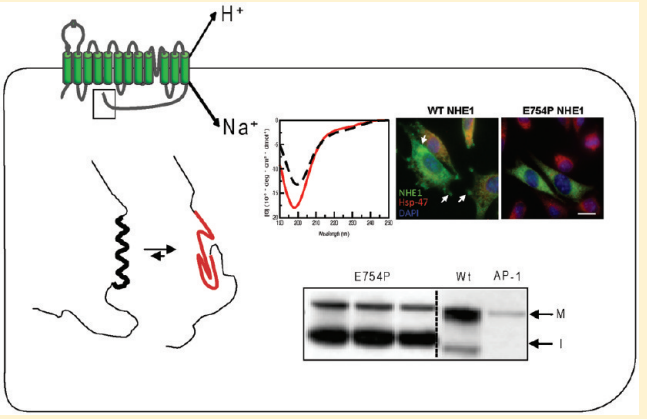

The ubiquitous plasma membrane Na^+/H^+ exchanger isoform 1 (NHE1, SLC9A1) plays central roles in cellular pH and volume homeostasis, cell migration, proliferation, and survival.[1] Altered NHE1 function is implicated in major clinical conditions such as cardiac ischemia−reperfusion damage and cancer development,[1] yet the reasons for NHE1 dysregulation in these pathological states remain incompletely understood. Membrane topology is conserved among the vertebrate NHEs[2−4] with 12 transmembrane helices and an intracellular C-terminal tail varying in length between species. The human (h) NHE1 C-terminal tail (*ct*) has 313 residues (V503−Q815), which can be functionally separated into a membrane proximal (*cpt*) (V503−T685) and a membrane distal domain (*cdt*) (V686−Q815). The *cpt* serves as a scaffolding platform with interaction sites for multiple proteins, including calmodulin,[5] calcineurin B homologous proteins (CHP) -1, -2, and -3,[6−8] and ezrin, radixin, and moesin (ERM) proteins.[9] The *cdt* contains numerous phosphorylation sites and is also implicated in protein−protein interactions, e.g., with Hsp70 and carbonic anhydrase II.[10,11] Despite this crucial role in NHE1 function and regulation, the structural organization of the full *ct* is sparsely described. A single far-UV circular dichroism (CD) analysis of the entire *ct* suggested the presence of a large fraction of coil structure,[12] and a small region (V503−H545) from the hNHE1*cpt* was shown to be α-helical in complex with either CHP-1 or -2.[6,8] Likewise, chemical cross-linking experiments suggest mobility within the C-terminal domain.[13] Given the functional importance of the *ct*, an understanding of the structural dynamics of this region could greatly facilitate advances in the understanding of NHE1 regulation and dysregulation.

Received: December 16, 2010
Revised: March 2, 2011
Published: March 22, 2011

The structure−function paradigm, i.e., that the structure of a protein determines its function,[14,15] has been challenged by the discovery of proteins that are intrinsically disordered (ID) yet fully functional.[15−17] The predicted occurrence of ID within the proteome is more frequent in eukaryotes than in prokaryotes and archaea,[18] likely reflecting the more complex cellular signaling and regulation in the former.[14] Very little is still known about the evolutionary conservation of ID.[19,20] However, it has been noted that local disorder in related ID proteins (IDPs) appears to be conserved to a greater extent than amino acid sequence, suggesting that in some cases disorder is the more important evolutionary constraint.[21]

ID provides flexibility for interactions with multiple partners. IDPs may recognize partners through local transiently formed structures termed molecular recognition features (MoRFs).[22,23] MoRFs are short segments of around 20 disordered residues or fewer, which are frequently involved in protein−protein interactions. These segments may undergo disorder-to-order transitions upon specific binding and often exist latently in low populations in the unbound state.[15,22,23] As part of their regulation ID regions are often phosphorylated with important functional consequences[24] as described for the glucocorticoid receptor, where phosphorylation of the activation domain leads to enhanced transcriptional activation.[25] Many membrane transport proteins, including NHE1, are highly regulated via multiple binding partners and phosphorylation sites. However, apart from a recent study of the *Drosophila melanogaster* Shaker K^+ channel that suggested a role for ID in protein−protein interactions,[26] the possible role of ID in regulation of ion transport is still unknown and has not experimentally been verified in the carrier class of transport proteins.

The aim of this study was first to investigate whether NHE1 has intrinsically disordered regions and to address the possible evolutionary conservation of such regions across vertebrate homologues of this carrier protein. Having established this, we investigated the possible functional roles of disorder in NHE1, focusing specifically on the role of conserved MoRFs within ID domains. We demonstrate that the *cdt* of NHE1 is intrinsically disordered and that the disordered region is evolutionarily conserved with retention of a specific disorder profile of local similarity. *In vitro* and *in vivo* analyses of a disrupted evolutionarily conserved motif within the ID region suggest that this transiently structured region is important for NHE1 trafficking. It is suggested that export from the endoplasmic reticulum (ER) may involve a transiently formed α-helix flanking an acidic ER-export motif.

EXPERIMENTAL PROCEDURES

Bioinformatics. The *cdt*s of NHE1 homologues from 15 species including teleost fishes, birds, amphibians, and mammals were aligned using ClustalW.[27] The sequences corresponding to the last two exons of hNHE1 was used: *Amphiuma tridactylum* (atNHE1; salamander, AAD33928, 44−45), *Xenopus laevis* (xlNHE1; clawed frog, NP_001081553, 24−25), *Mus musculus* (mmNHE1; mouse, Q61165, 35−36), *Rattus norvegicus* (rnNHE1; rat, P26431, 35−36), *Cricetulus griseus* (cgNHE1; Chinese hamster, P48761, 35−36); *Sus scrofa* (ssNHE1; pig, P48762, 34−35), *Bos taurus* (btNHE1; cow, Q28036, 34−35), *Homo sapiens* (hNHE1; human, P19634, 34−35), *Oryctolagus cuniculus* (ocNHE1; rabbit, P23791, 34−35), *Gallus gallus* (ggNHE1; chicken, ABB82239, 23−24), *Takifugu rubripes* (trNHE1; Japanese pufferfish, BAE75800, 19−20), *Pleuronectes americanus* (paNHE1; winter flounder, AA044956, 40−41), *Platichthys flesus* (pfNHE1; European flounder, CAB45141, 39−40); *Oncorhynchus mykiss* (omβNHE1; rainbow trout, AAA49549, 29−30), and *Cyprinus carpio* (ccNHE1; carp, CAB45232, 16−17). These sequences were retrieved from UniProtKB at EMBL, EBI (101) and NCBI (102) and accession numbers listed. The numbering of the sequences and positions includes the entire sequence containing the signal sequence. The last two numbers in the parentheses are the suggested signal peptide cleavage site obtained from SignalP3.0.[28] Alignment by ClustalW of only hNHE1*cdt* with paNHE1*cdt* was also performed.

Cloning and Site-Directed Mutagenesis. The NHE1 C-terminal distal tails were cloned as Met + paNHE1-(V674−S779) (paNHE1*cdt*) and Met + hNHE1(V686-Q815) (hNHE1*cdt*) in a pET11.a vector (Novagen). Primers were designed to amplify the DNA constructs (restriction sites are underlined and denoted in brackets): paNHE1*cdt* forward primer: 5′-ATCATATGGTCCCTGCCAATCG-3′ [NdeI], reverse primer: 5′-GAGGATCCTCATGAGACGAAG-3′, [*Bam*HI], hNHE1*cdt* forward primer: 5′-TACCATATGGTGCCAGCCC-3′ [NdeI], reverse primer: 5′-GTGGCTAGCTCACTGCCCCTTG-GGGAAG-3′ [NheI]. The plasmids were purified using the Wizards plus SV miniPrep DNA purification system (Promega, Madison, WI). The mutant protein paNHE1*cdt*^{E754P} was prepared from the paNHE1*cdt* plasmid using a QuikChange II Site-Directed Mutagenesis Kit (Stratagene) with the following primers: paNHE1cdt^{E754P} forward: 5′-GACGACCAGGAGCCGCAACTGAAACTATCC-3′; paNHE1cdt^{E754P} reverse: 5′-GGATAGTTTCAGTTGCGGC-TCCTGGTCGTC-3′. Constructs were confirmed by sequencing (Eurofins MWG Operon, Ebersberg, Germany).

Preparation and Expression of the Full-Length paNHE1 Mutant. The full length mutant paNHE1^{E754P} was prepared from a C-terminally His-tagged WT paNHE1 in pcDNA3.1(+), using QuickChange XL Mutagenesis kit (Stratagene) and the same mutagenic primer sequences described for the preparation of the corresponding *cdt*. The construct was verified by DNA sequencing (Eurofins MWG Operon, Ebersberg, Germany) prior to Lipofectamine 2000-mediated transfection into AP-1 cells, a mammalian cell line lacking endogenous NHE activity.[29,30] Positive transfectants were selected for resistance to 600 μg/mL G418. NHE1 expression was verified by immunoblotting, as described in ref 4.

h- and paNHE1cdt Production and Purification. Recombinant hNHE1*cdt*, paNHE1*cdt*, and variant were obtained as described.[31] The purity of all protein preparations was >95% as judged by SDS-PAGE analysis.

CD Spectroscopy. Far-UV CD measurements were recorded on a Jasco J-810 spectropolarimeter with Peltier control at 20 °C using 1 mm path length from 250 to 190 nm with a scan speed of 20 nm/min, 5 or 10 scans, on 8 or 10 μM protein in 20 mM NaH_2PO_4, pH 7.0. Spectra were buffer corrected and smoothed.

NMR Spectroscopy. For backbone assignments 1.1 mM protein samples of both the $^{15}N,^{13}C$-paNHE1*cdt* and $^{15}N,^{13}C$-hNHE1*cdt* in PBS (8 g/L NaCl, 0.2 g/L KCl, 1.78 g/L $Na_2HPO_4 \cdot H_2O$, 0.24 g/L KH_2PO_4), pH 7.0, were used including 40 μM 4,4-dimethyl-4-silapentane-1-sulfonic acid (DSS), 10 mM dithiothreitol (DTT), and 10% (v/v) 99.96% D_2O. For measurements of ^{15}N relaxation, 0.5 mM ^{15}N-labeled proteins in the same buffer were used. All NMR spectra were recorded on a Varian INOVA 750 MHz ^1H NMR spectrometer equipped with a 5 mm triple resonance probe with a *Z*-field gradient at 4 °C. The following experiments were recorded for

hNHE1*cdt* and paNHE1*cdt*—[^{1}H,^{15}N]-HSQC, HNCA,[32] HN(CO)CA,[33] HNCACB,[34] CBCA(CO)NH,[35] HNCO,[32] and HN(CA)CO[36]—and used for backbone assignments. For assignments of C^{α} and C^{β} chemical shifts of the mutant protein, only HNCACB and CBCA(CO)NH spectra were recorded. Spectra were transformed using NmrPipe[37] and analyzed with CCPNMR Analysis 1.0.[38] AutoAssign[39] was used to aid backbone assignment. C^{α} and C^{β} chemical shifts obtained at 4 °C were used for secondary structure propensity (SSP) analysis.[40] Proton chemical shifts were referenced directly to internal DSS at 0.00 ppm, with heteronuclear dimensions referenced indirectly using their relative gyromagnetic ratios.[41]

The ^{15}N spin relaxation experiments included determination of the longitudinal (R_1) and transverse (R_2) relaxation rate constants and were recorded using a standard HSQC sequence at a 750 MHz proton frequency field at 4 °C. The relaxation decays were measured using a six step relaxation delay for paNHE1*cdt* R_1 (0, 0.2, 0.4, 0.6, 0.6, 0.8, and 1.0 s), a seven-step relaxation delay for hNHE1*cdt* R_1 (0, 0.2, 0.4, 0.6, 0.6, 0.8, 1.0, and 1.2 s) and a seven-step relaxation delay (0.01, 0.05, 0.09, 0.13, 0.17, 0.21, and 0.25 s) for R_2 of both hNHE1*cdt* and paNHE1*cdt*. The number of transients was 64 for paNHE1*cdt* and 32 for hNHE1*cdt* experiments, and the number of increments was 32 for paNHE1*cdt* and 57 for hNHE1*cdt* experiments. Longitudinal and transverse relaxation times were calculated in CCPNMR analysis by fitting the height of each peak to a single-exponential decay function, and each fit was manually reviewed. Error bars were calculated as errors of the fit. The relaxation rates were determined at 0.5 mM protein in PBS (8 g/L NaCl, 0.2 g/L KCl, 1.78 g/L $Na_2HPO_4 \cdot H_2O$, 0.24 g/L KH_2PO_4), pH 7.0, 40 μM DSS, 10 mM DTT, and 10% (v/v) 99.96% D_2O.

Small-Angle X-ray Scattering. Samples for SAXS analyses were in PBS buffer, pH 7.0. Data were recorded on the X33 beamline at EMBL, Hamburg, using an exposure time of 2 min. Data were recorded on 1:1, 2:3, and 1:3 dilutions of a stock with a protein concentration of 0.66 mM (paNHE1*cdt*) and 0.71 mM (hNHE1*cdt*).[31]

Full-Length paNHE1 Mutant. AP1 cells[30] were a kind gift from S. Grinstein, University of Toronto. After exogenous expression of NHE1, their rate of recovery from acid loading in the absence of HCO_3^- is a measure of NHE1 activity.[29] Cells were maintained at 5% CO_2, 37 °C, in α-minimal essential Eagles medium with 10% FBS, 1% penicillin/streptomycin, and 600 μg/mL G418 (Invitrogen) as described.[4,29] NHE1 protein expression was verified by immunoblotting,[4] using a mouse monoclonal NHE1 antibody (Milipore/Chemicon). NHE1 function was assayed at 37 °C, as described,[4,29] using the fluorescent, pH-sensitive probe 2′,7′-bis(2-carboxyethyl)-5,6-carboxy-fluorescein (BCECF-AM). Coverslips were mounted in a fluorescence photometer (PTI, Lawrenceville, NJ) and perfused with Hepes Ringer (HR; in mM: 130 NaCl, 3 KCl, 20 HEPES, 1 $MgCl_2$, 0.5 $CaCl_2$, 10 NaOH, 10 glucose; pH 7.4). The NH_4Cl prepulse elicited a similar degree of acidification in AP1 cells expressing WT and mutant NHE1, consistent with intrinsic buffering capacities being similar in the pH range studied. The rate of pH_i recovery was always calculated from similar starting pH_i values.

Analysis of NHE1 Function. The AP-1 cells were exposed to an NH_4Cl prepulse (10 mM, in HR), followed by perfusion with Na^+-free HR (Na^+ replaced by $NMDG^+$). BCECF ratio was calibrated to pH_i using a seven-point high KCl/nigericin calibration.[29] Data were quantified as the initial rate of pH_i recovery in pH units/min. Immunofluorescence analysis was carried out essentially as in ref 4. The cells were co-labeled using a polyclonal rabbit NHE1 antibody (a kind gift from Mark Musch, University of Chicago) and mouse monoclonal antibodies against the ER marker Hsp47 (Enzo Life Sciences, Plymouth Meeting, PA), the late endosome/lysosome marker Lamp-1 (sc-20011, Santa Cruz Biotechnology, Santa Cruz, CA), cytochrome *c* (Becton-Dickinson Pharmingen) to label mitochondria, and giantin (Abcam, Cambridge, UK) to label the Golgi apparatus. Secondary antibodies employed were goat antirabbit Alexa488 and goat antimouse Alexa568, and nuclei were stained using DAPI. Preparations were analyzed using the 100×/1.4 NA objective of a Leica DMIRB/E microscope with a confocal laser-scanning unit (TSC NT; Leica) or the 100×/1.4 NA objective of an Olympus Bx63 epifluorescence microscope, as indicated. No or negligible labeling was seen in the absence of primary antibody or in untransfected AP1 cells. Images were processed (overlays and brightness/contrast adjustment only) using Adobe Photoshop software.

Table 1. Sequence Conservation between NHE1 Sequences[a]

	all species[b]	tetrapods	teleosts
ct[c]			
% identity	65.2	84.3	65.3
% similarity	71.7	88.0	72.2
cpt[d]			
% identity	77.5	92.8	72.5
% similarity	84.2	95.8	80.3
cdt[e]			
% identity	51.2	74.5	58.1
% similarity	57.8	79.8	63.4

[a] Numbers are calculated using the online algorithm SIAS (http://imed.med.ucm.es/Tools/sias.html). [b] The sequences used in Figure 1 are compared. [c] The *ct* is defined from residue 500 (hNHE1) and out (residue 815 hNHE1). [d] The *cpt* covers the intracellular tail up to exon 10. [e] The *cdt* covers the last two exons, exons 11 and 12.

RESULTS

The NHE1 C-Terminal Distal Tail Shows Conservation of Intrinsic Disorder across a Wide Range of Vertebrate Species. Initially we compared the sequences of NHE1 from 15 representative homologues from teleost fishes, birds, amphibians, and mammals (Table 1). Sequence identity was higher (~80%) in the *cpts* than in the *cdts* (~50%) as has been noted before.[42] Alignment of the *cdts* of the 15 species shows that when divided into two groups representing the tetrapods and the teleost fishes, the sequence identity rose dramatically within each group (Figure 1, Table 1). Two motifs were fully conserved between all the homologues: the sequences YLTVPA (hNHE1 Y683−A688), named the TV box, and RCLSDPGP (hNHE1 R793-P800), hereafter the LSD box. In the present paper we define the border between the *cpt* and the *cdt* to be after the calmodulin binding sites[5] and after a predicted α-helix. The two parts divide the TV box in half such that the hNHE1*cdt* starts at V686.

In silico analysis of the presence and conservation of ID in the NHE1*ct* for all 15 species revealed that the *cpts* are predicted to be largely folded (data not shown), whereas the *cdts* are predicted to possess a high degree of disorder (see below, Figure 2A upper panel, and Supporting Information Figure S1). We therefore analyzed disorder in the *cdt* experimentally by comparing two

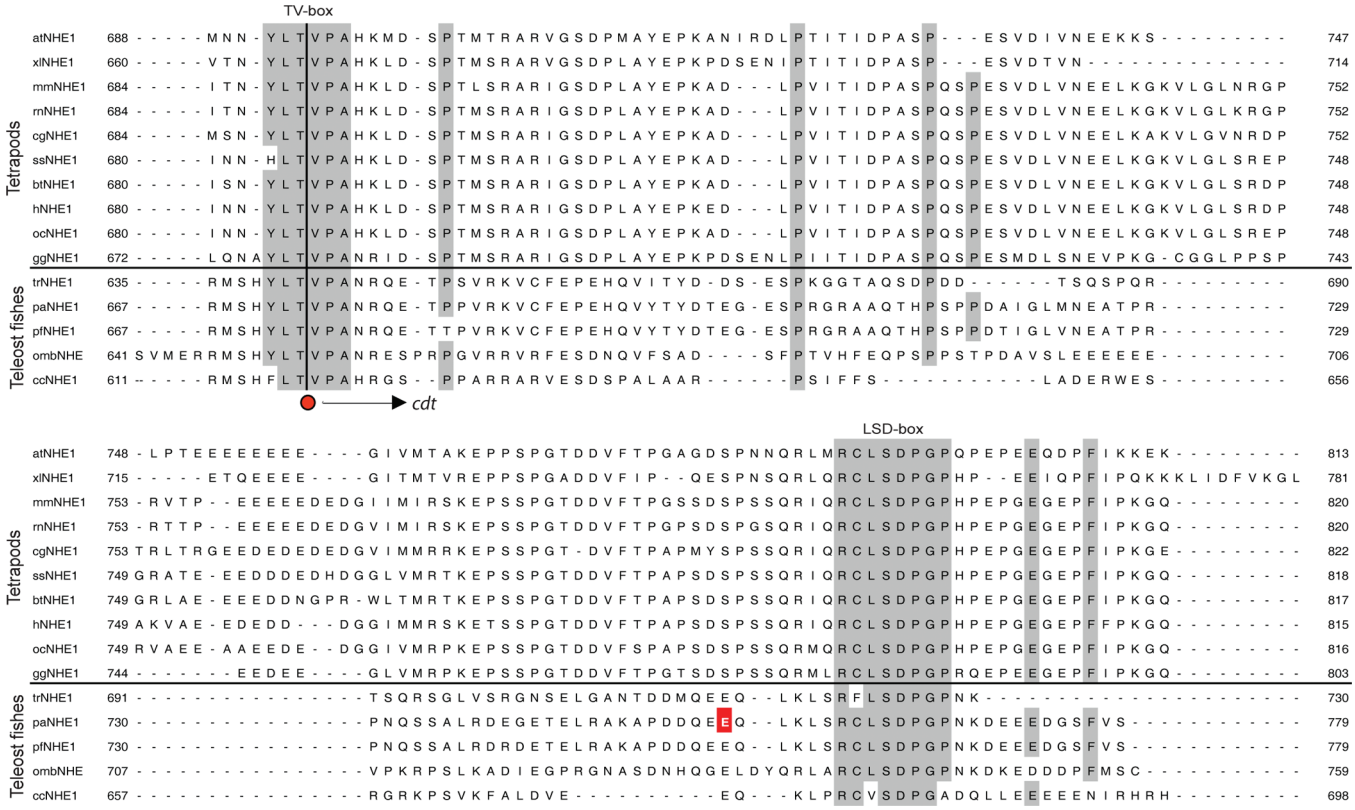

Figure 1. Multiple sequence alignment of the NHE1 C-terminal distal tail (*cdt*) from the following 15 species (for accession numbers, see Supporting Information Materials and Methods): *Amphiuma tridactylum* (atNHE1; salamander), *Xenopus laevis* (xlNHE1; clawed frog), *Mus musculus* (mmNHE1; mouse), *Rattus norvegicus* (rnNHE1; rat), *Cricetulus griseus* (cgNHE1; Chinese hamster); *Sus scrofa* (ssNHE1; pig), *Bos taurus* (btNHE1; cow), *Homo sapiens* (hNHE1; human), *Oryctolagus cuniculus* (ocNHE1; rabbit), *Gallus gallus* (ggNHE1; chicken), *Takifugu rubripes* (trNHE1; Japanese pufferfish), *Pleuronectes americanus* (paNHE1; winter flounder), *Platichthys flesus* (pfNHE1; European flounder); *Oncorhynchus mykiss* (omβNHE1; rainbow trout), and *Cyprinus carpio* (ccNHE1; carp). paNHE1 E754 is highlighted (red box).

evolutionarily distant species: human NHE1 (hNHE1) and *Pleuronectes americanus* (paNHE1; winter flounder). There were several reasons for this choice: hNHE1 and paNHE1 share several mechanisms of regulation,[43,44] yet they function at different temperatures and osmotic environments and they are evolutionarily distant and represent each of the two subgroups in Figure 1. Thus, if both are disordered, this indicates that ID could serve an essential functional role in NHE1.

IDPs have hydrodynamic properties, sequence composition, and biophysical characteristics that are distinct from those of globular proteins.[45−48] To evaluate the potential presence of such properties in NHE1, we first analyzed the distribution of structure and disorder in hNHE1*ct* using *in silico* predictions. All disorder algorithms tested predicted the presence of ID in the hNHE1*cdt* (Figure 2A, top) with small stretches of secondary structure suggested from order algorithms, albeit all of these with small amplitudes (Figure 2A, bottom).

For experimental validation of the disorder, we produced the constructs hNHE1*cdt* (V686-Q815) and paNHE1*cdt* (V674−S779) corresponding to the outermost C-terminal part of the intracellular tail of hNHE1 and paNHE1, respectively. The purity of the recombinant protein preparations were assessed from SDS-PAGE gels stained with Coomassie Brilliant Blue (Supporting Information Figure S3). The samples were all of high purity (>95%). The two constructs were designed to include the region of predicted disorder, and although the intracellular parts of the two transporters are of different length, they align within the TV box and the LSD box (Figure 1). The small-angle X-ray scattering (SAXS) profile did not exhibit signs of aggregation even at high concentration and based on the intensity of the scattering the molecular mass of the particles were estimated to 10 and 11 kDa for hNHE1*cdt* and paNHE1*cdt*, respectively. The small deviation from the theoretical molecular weight most likely reflects the uncertainty in the determination of the protein concentration due to the low extinction coefficients. The SAXS measurement thus demonstrates that the recombinant proteins are monomeric and suited for biophysical analysis. When presented as a Kratky plot, the SAXS profile of hNHE1*cdt* increased throughout its range (Figure 2C), a pattern characteristic for unfolded proteins.[49] The secondary structure and overall fold analyses of hNHE1*cdt* by far-UV CD spectroscopy showed a distinct minimum at ∼200 nm and a shoulder at 220−230 nm, indicating the absence of regular secondary structures (Figure 2B).[31] Finally, the [^{1}H,^{15}N]-HSQC NMR spectrum of hNHE1*cdt* showed a significant lack of dispersion in the proton dimension (Figure 2D), demonstrating in unison with the other data that the regulatory distal domain of NHE1 is intrinsically disordered. To experimentally verify the apparent evolutionary conservation of disorder in the NHE1*cdt*, paNHE1*cdt* was then subjected to the same analyses as hNHE1*cdt* and was found to show the same predicted and experimental characteristics of ID (Supporting Information Figure S2). Lastly, the apparent evolutionary conservation of ID in NHE1 was substantiated by *in silico* disorder

dx.doi.org/10.1021/bi1019989 |*Biochemistry* 2011, 50, 3469–3480

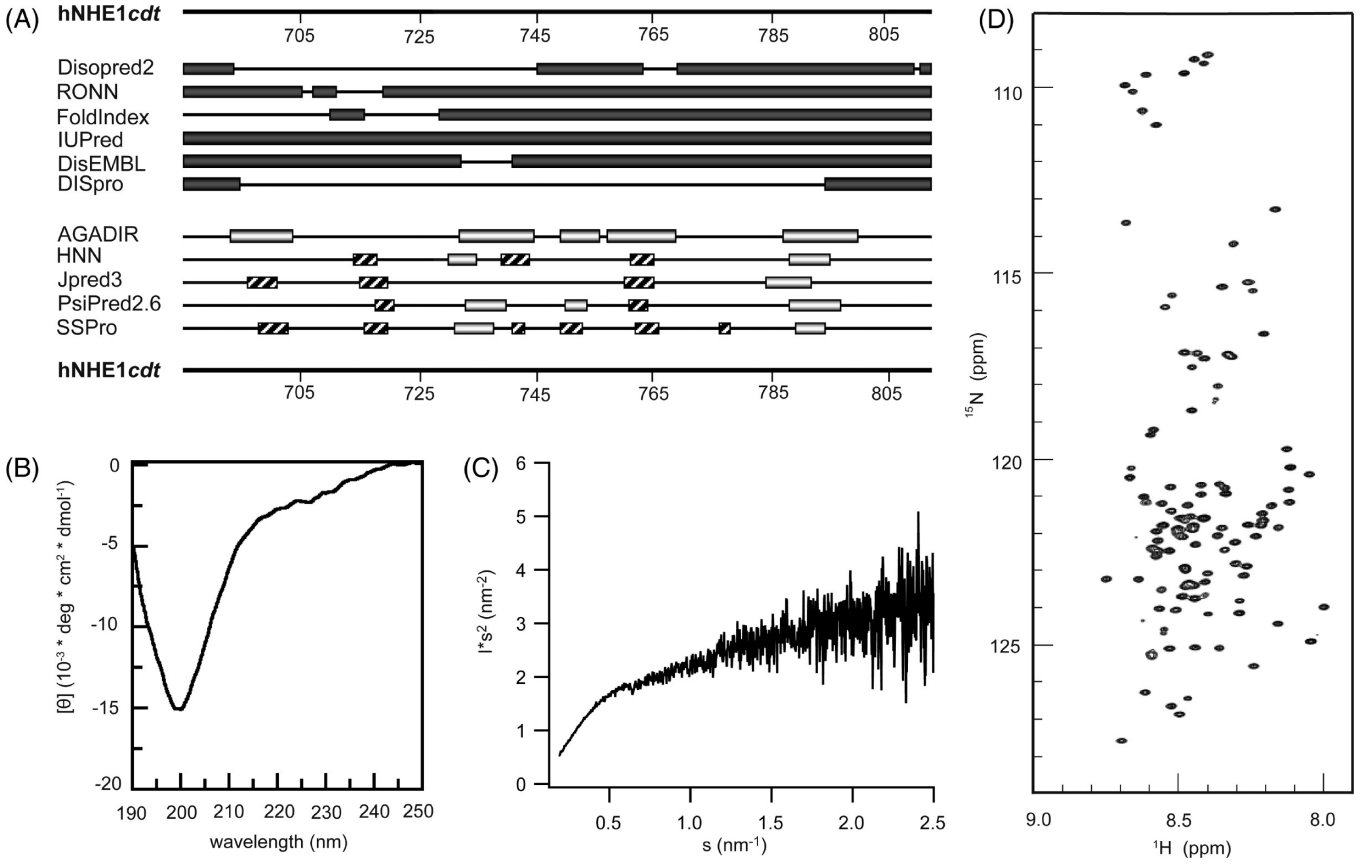

Figure 2. hNHE1*cdt* is intrinsically disordered. (A) Structure and disorder predictions by various algorithms; disorder (black), α-helix structure (gray), β-strand structure (hatched). (B) Far-UV CD spectrum of 8 μM hNHE1*cdt* in 20 mM NaH_2PO_4 pH 7.0 at 20 °C. (C) Kratky plot of SAXS data. (D) [^{1}H,^{15}N]-HSQC of 1.1 mM ^{13}C−^{15}N-labeled hNHE1*cdt* in PBS buffer, pH 7.0 recorded at 4 °C.

predictions for the *cdt*s of all 15 NHE1 homologues (Supporting Information Figure S1).

Taken together, substantial experimental data on two distant homologues of the NHE1 supported by *in silico* predictions on the entire set of sequences strongly indicate that the intracellular distal tail of NHE1 is intrinsically disordered and that this property is evolutionarily conserved among vertebrate NHE1s.

Regions of Transient Secondary Structure Are Conserved in the NHE1*cdt*. Regions of structural disorder frequently have segments of transient secondary structure, which are thought to be important e.g. in mediating protein−protein interactions.[23] Therefore, we next employed NMR spectroscopy to characterize the dynamics and secondary structure propensity (SSP) of the h- and paNHE1*cdt*s at the residue level. Since the chemical shifts of IDPs are often close to their random coil values,[40] analyses of structure relating to these values can be difficult to interpret. One method for evaluating SSP in IDPs was applied, in which the ^{13}C chemical shifts are incorporated into a single residue specific SSP score.[40] SSP scores can range from +1 for fully formed α-helix to −1 for fully formed β-strand. Values close to zero indicate the absence of secondary structures, and intermediate values indicate that the secondary structures are only transiently populated with amplitudes relating to the SSP value. The C^{α} and C^{β} chemical shifts of paNHE1*cdt* and hNHE1*cdt* were assigned and analyzed, and SSP scores were calculated for all residues in the *cdt*s of the two transporters (Figure 3). The SSP scores were aligned using a ClustalW sequence alignment. For hNHE1*cdt* three areas of transient α-helix formation (H) with SSP scores higher than 0.1 were observed: S729−L744 ($H1_h$), G760−S770 ($H2_h$), and P786−P798 ($H3_h$). Four stretches exhibited negative SSP scores, suggesting extended structures (S) in these regions, namely, V716−E728 ($S1_h$), S745−G760 ($S2_h$), F778−S785 ($S3_h$), and G805−Q815 ($S4_h$).

The SSP analysis of paNHE1*cdt* revealed two regions of transient α-helicity: G721−A726 ($H1_{pa}$) and D751−P765 ($H2_{pa}$), which coincided with the $H1_h$ and $H3_h$ regions in hNHE1 although with different amplitudes of the SSP scores (Figure 3). Notably, paNHE1*cdt* lacks $H2_h$, possibly indicating the presence of a regulatory element in hNHE1 not found in paNHE1 (see Discussion). Four areas in paNHE1*cdt* had negative SSP scores: E690−D699 ($S1_{pa}$), T727−Q732 ($S2_{pa}$), A746−D750 ($S3_{pa}$), and G766−G775 ($S4_{pa}$), suggesting extended conformation in these areas. $S3_{pa}$ coincided with $S3_h$ while the others had no direct parallels in hNHE1*cdt*. The most striking similarity in SSP scores between the hNHE1*cdt* and the paNHE1*cdt* is in the region containing $S3_h$/$S3_{pa}$ and $H3_h$/$H2_{pa}$. Remarkably, sequence identity in this region is low, except within the LSD box.

Collectively, these date indicate that both proteins adopts regions of transient structure mainly of α-helical character. Surprisingly, despite low sequence identity, these regions coincide but have variable amplitudes. Thus, explicit functions relating to the basal function of the transporter may be encoded in the coinciding and conserved regions whereas specialized function may reside in the nonoverlapping sites.

Backbone Dynamics of hNHE1*cdt* and paNHE1*cdt* Supports the SSP Analyses. The dynamics of hNHE1*cdt* and

dx.doi.org/10.1021/bi1019989 |*Biochemistry* 2011, 50, 3469–3480

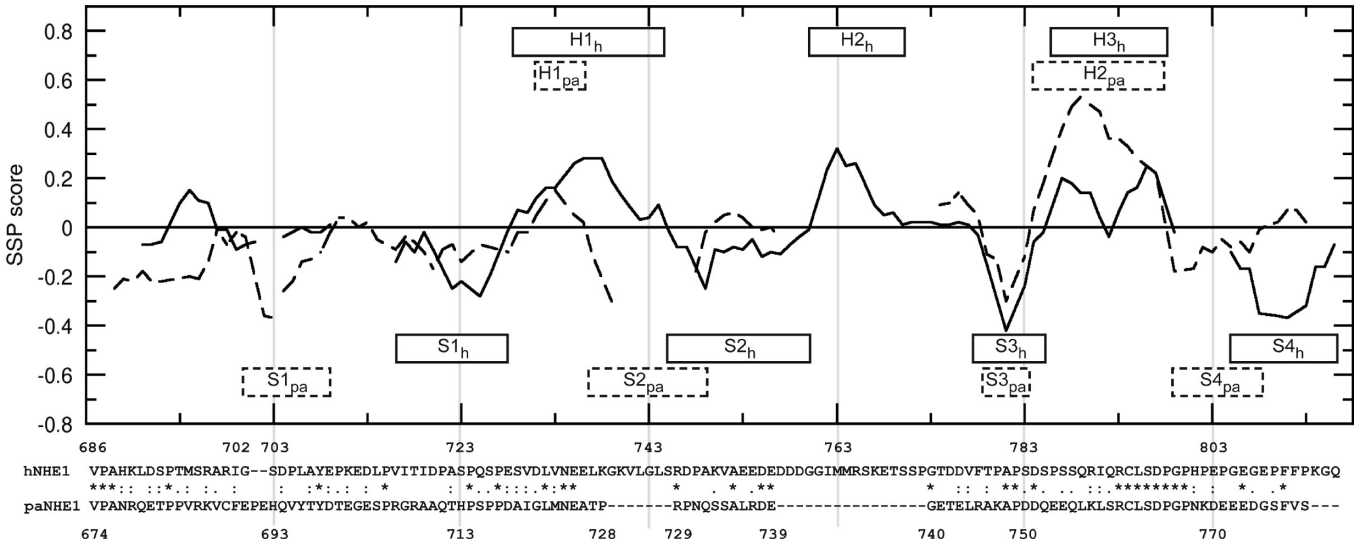

Figure 3. Secondary structure propensity (SSP) analyses from chemical shifts of hNHE1*cdt* and paNHE1*cdt*. The SSP scores identify regions of transient structure formation in the ID region from chemical shifts of C^{α} and C^{β}. These were obtained at 4 °C were used for SSP analyses of hNHE1*cdt* (solid line) and paNHE1*cdt* (dashed line) and aligned using a ClustalW sequence alignment (bottom). Gray lines relate sequence numbers of the intact proteins to the SSP. Differences in SSP of the N-terminal parts of hNHE1*cdt* and paNHE1*cdt* were disregarded in the comparison since influence from the *cpt* cannot be neglected. Boxes (solid hNHE1*cdt*; dashed paNHE1*cdt*) indicate potential MoRFs (see text for details).

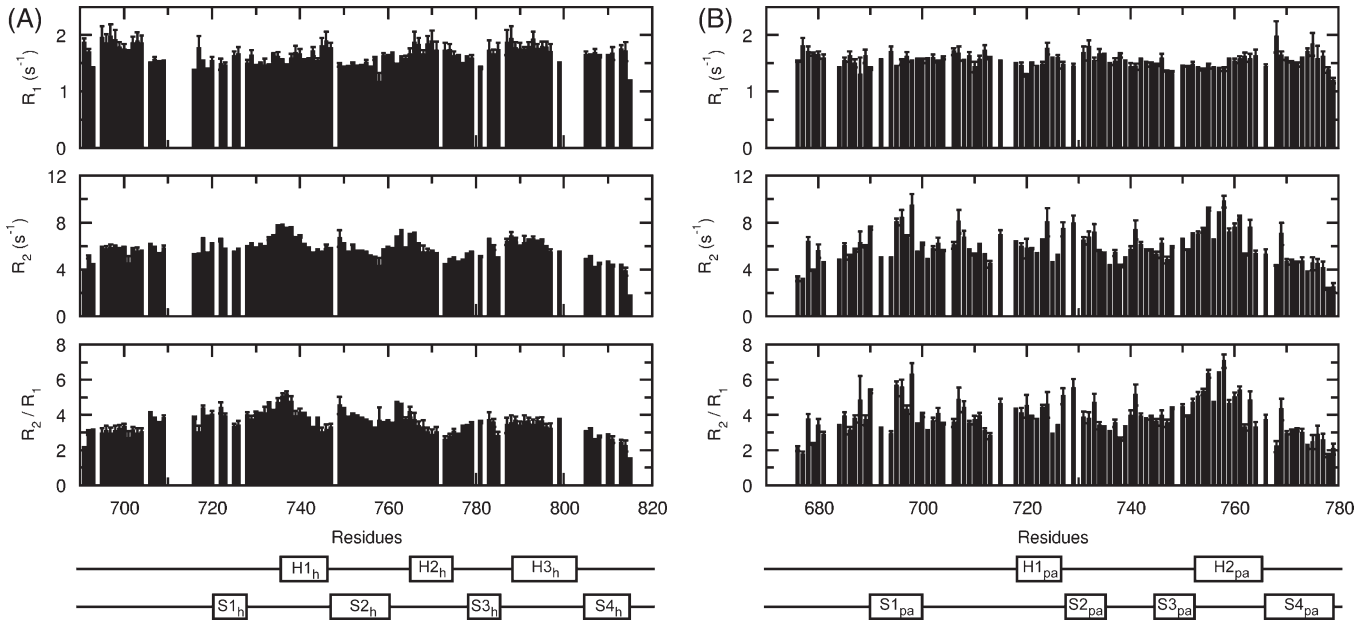

Figure 4. hNHE1*cdt* and paNHE1*cdt* ^{15}N relaxation data show slower dynamics in the transient α-helix regions. The reciprocal values of T1 and T2 (R_1 and R_2) and the R_2/R_1 ratios were plotted for each residue for (A) hNHE1*cdt* and (B) paNHE1*cdt*. Error bars indicate standard errors of the fit. Missing data points are either due to prolines or unassigned residues. The potential MoRFs derived from the SSP analyses (Figure 3) are shown.

paNHE1*cdt* were further characterized using ^{15}N relaxation analyses (Figure 4). The larger R_2/R_1 ratios and R_2 values correspond to regions with restricted backbone mobility on the picoseconds to nanoseconds time scale, i.e., often corresponding to more structured regions, whereas smaller R_2/R_1 ratios and R_2 values indicate more backbone mobility, i.e., often corresponding to more unfolded regions.[50] For both, the h- and paNHE1*cdt*, fast dynamics (low R_2/R_1 ratios <6) were generally observed for the entire chain, underscoring the lack of stable structures. The hNHE1*cdt* exhibited three regions of elevated R_2 compared to average and thus slower dynamics. These were S729−L744, G759−S770, and P786−P798 (Figure 4A), directly corresponding to $H1_h$, $H2_h$, and $H3_h$ as identified by the SSP analysis. In paNHE1*cdt* (Figure 4B), two areas exhibited elevated R_2 values, E690−T700 and D751−P765, the latter corresponding to $H2_{pa}$. For most regions for which extended structure was indicated in the SSP analysis (Figure 3), no elevated R_2 values were observed, suggesting statistical coil-like dynamics.

The ^{15}N relaxation data are thus in accordance with the general conclusion that the NHE1*cdt* exhibits ID and support

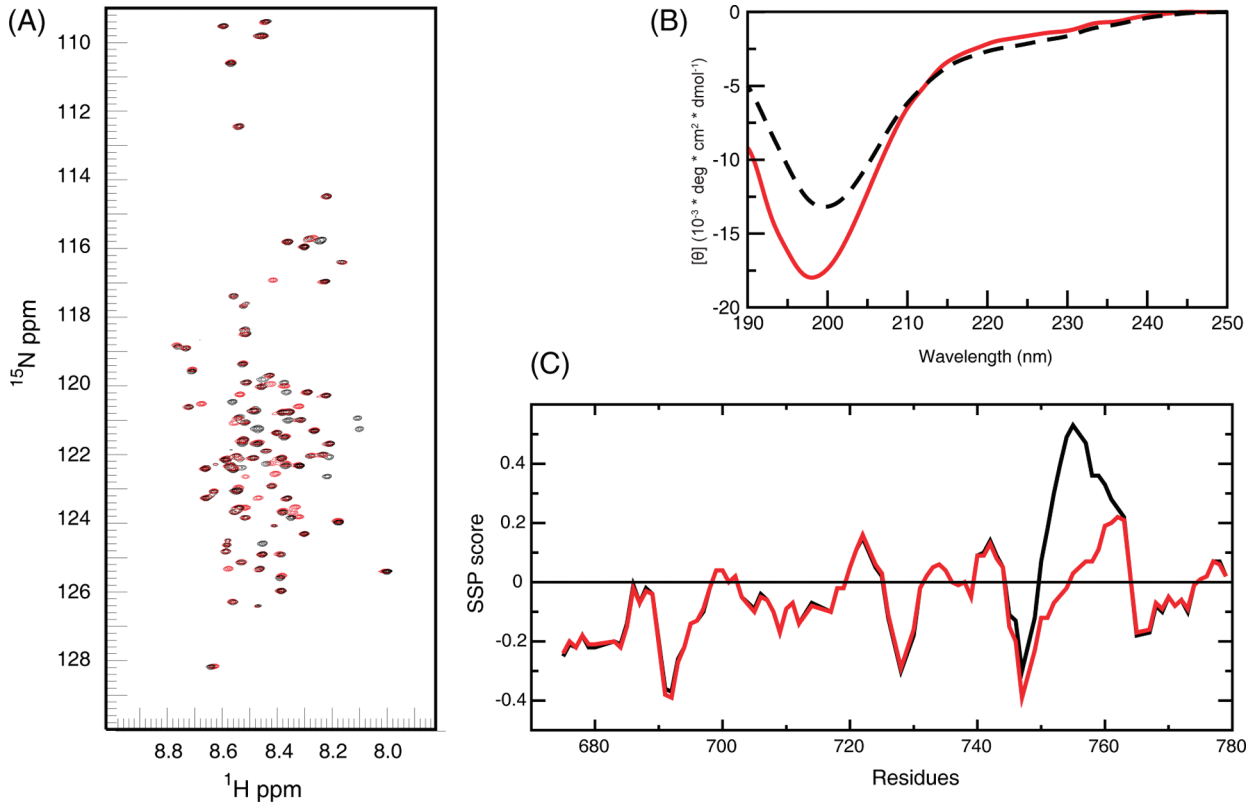

Figure 5. Disorder characterization of the paNHE1*cdt*^{E754P} mutant. (A) Comparison of [^{1}H,^{15}N]-HSQC spectrum of 1.1 mM ^{13}C−^{15}N-labeled WT paNHE1*cdt* (black) and paNHE1*cdt*^{E754P} mutant (red) in PBS buffer, pH 7.0 recorded at 4 °C. Lowers dispersion in the proton dimension is observed for the mutant protein. (B) Far-UV CD spectrum of 10 μM paNHE1*cdt* (dashed black) and 10 μM paNHE1*cdt*^{E754P} mutant (solid red) in 20 mM NaH_2PO_4 pH 7.0 at 20 °C, showing a distinct unfolding of the mutant with lower absorption at 222 nm and increased absorption below 200 nm. (C) SSP analyses from chemical shifts of paNHE1*cdt* (black) and paNHE1*cdt*^{E754P} (red). A significant disruption of the major MoRF is apparent from the SSP analyses.

the conclusion from the SSP analyses that structures are formed mainly in the form of transient α-helices. These transiently structured regions with more restricted dynamics are conserved between the species.

Disruption of a Conserved MoRF. The above findings that ID and transient secondary structure in the NHE1*cdt* are evolutionarily conserved suggested to us that these properties are likely to serve important and common physiological roles. To begin to address this experimentally, we targeted $H2_{pa}$ (D751−G766), which had the largest positive SSP score of all regions studied in the two NHE1s and coincided with $H3_h$, suggesting a conserved functional role. We scanned the entire MoRF *in silico* by proline substitutions and compared the resultant structure propensities using Agadir.[51] The most severe effect was obtained for the mutation E754P where the MoRF was suppressed to 0.28%^{E754P} vs 13.7%^{WT} for the wilds type (theoretical average of the D751−G766 peptide). We note that the E754 is nonconserved in the 15 sequences of NHE1. The E754P mutation was introduced into paNHE1*cdt*, creating paNHE1*cdt*^{E754P}. Comparison of the [^{1}H,^{15}N]-HSQC of paNHE1*cdt*^{E754P} with that of WT showed distinct differences in chemical shift dispersion (Figure 5A), and the CD spectra were distinctly different, supporting less structure in the variant (Figure 5B). The C^{α} and C^{β} chemical shifts of paNHE1*cdt*^{E754P} were assigned and used for SSP analysis which was compared to the SSP profile of WT (Figure 5C). Consistent with the *in silico* prediction, paNHE1*cdt*^{E754P} showed a significant decrease in average SSP score—i.e., a reduction in α-helix propensity—to an average of −3.5%, compared to an experimental value of 27.5% for WT (average of D751−G766). Thus, the ability of $H2_{pa}$ to form a helix was successfully disrupted by this single mutation.

Disruption of a Conserved MoRF Alters NHE1 Glycosylation and Activity after an Acid Load. To investigate the role of the main conserved MoRF, $H2_{pa}$, for the function of NHE1*cdt*, we next transferred the E754P mutation to full-length paNHE1. The construct was stably transfected into AP-1 cells, which lacks endogenous NHE1 activity.[4,30,44] The total expression level was comparable to that of WT, but the relative amount of mature, fully glycosylated NHE1 was greatly reduced with a corresponding increase in the core-glycosylated, immature NHE1 (Figure 6A). This suggested that a large fraction of the NHE1 protein might be defectively trafficked and thus intracellularly localized.[52] To further address this issue, we next tested whether plasma membrane NHE1 function was impaired in cells expressing the mutant NHE1. As previously shown, the rate of pH_i recovery after an NH_4Cl-prepulse-induced acid load in AP1 cells in the nominal absence of HCO_3^- reflects the activity of the exogenously expressed NHE1.[29] As seen in Figure 6B,C, NHE1 activity after acid loading in cells transfected with paNHE1^{E754P} was about half of that in cells expressing WT NHE1.

Disruption of a Conserved MoRF Results in Reduced NHE1 Plasma Membrane Targeting. Given the similar overall expression levels of WT paNHE1 and paNHE1^{E754P} and the reduced glycosylation of the latter, the reduced NHE1 activity

dx.doi.org/10.1021/bi1019989 |*Biochemistry* 2011, 50, 3469–3480

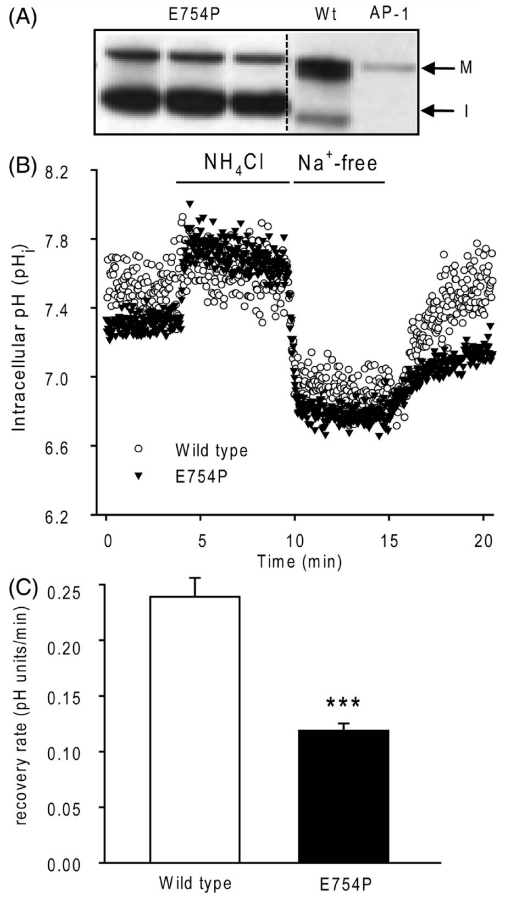

Figure 6. The paNHE1^{E754P} mutation is associated with reduced plasma membrane NHE1 function and apparent reduction in NHE1 glycosylation. (A) Western blots of NHE1 expression. From left: AP1 cells stably expressing paNHE1^{E754P} (n = 3), WT paNHE1, and untransfected AP-1 cells (all from same blot, which was cut at the hatched line to omit irrelevant wells). Predominantly, WT paNHE1 is in the fully glycosylated, ~100 kDa form (M), while the mutant is in the immature ~85 kDa form (I). (B) AP-1 cells expressing WT or paNHE1^{E754P} were loaded with the fluorescent, pH-sensitive probe BCECF, and the recovery of pH_i after an NH_4Cl-prepulse-induced acid load monitored. The cells were perfused with HR solution, or, where indicated by the bar, with HR +10 mM NH_4Cl or with Na^+-free HR (Na^+ replaced by $NMDG^+$). The traces are representative of 5 (WT) or 4 (paNHE1^{E754P}) independent experiments. (C) The experiments shown in (B) were summarized by calculating the pH_i recovery rate in pH units/min from the initial, linear part of the curve after reintroduction of Na^+. Data are mean values with SEM error bars. n = 5 (WT) and 4 (paNHE1^{E754P}) independent experiments per cell type. (***) The value is significantly different from that in cells expressing WT paNHE1 (Students t test, $p < 0.001$).

of the mutant seemed most likely to reflect altered targeting to the plasma membrane or altered activity of the NHE1 proteins at the plasma membrane. To distinguish between these possibilities, immunofluorescence labeling and confocal imaging were performed to determine if the mutation disrupted NHE1 plasma membrane targeting. WT paNHE1 exhibited the pattern previously reported for NHE1[53] with plasma membrane localization especially to membrane protrusions (Figure 7A–C, white arrows; Figure 7E) but also punctuate intracellular localization. The NHE1^{E754P} mutant clearly exhibited reduced plasma membrane localization compared to that of WT NHE1. A fraction of both mutant and WT NHE1 appears to localize to late endosomes/lysosomes (Figure 7A), as would be expected from general turnover of the protein, with no detectable differences in this localization between WT and mutant NHE1. Finally, the NHE1^{E754P} mutant appeared to exhibit markedly increased ER localization compared to WT NHE1 (Figure 7B), consistent with previous reports that core-glycosylated-only NHE1 is primarily found in the ER.[52] In contrast, neither WT nor mutant NHE1 appeared to co-localize with mitochondria (Figure 7C), and while some Golgi localization of immature NHE1 is of course expected, the overall localization pattern differed greatly from that of Golgi (Figure 7D).

Collectively, these findings indicate that the E754P mutation interferes with NHE1 export to the plasma membrane possibly via accumulation in the ER, resulting in detectable nonmature glycosylation and reduced NHE1 levels at the plasma membrane.

DISCUSSION

The main conclusion from this study is that the intracellular distal tail of NHE1 from two evolutionarily distant species, winter flounder and human, are intrinsically disordered and that the structure propensity profiles exhibit substantial similarities between the two species. In conjunction with *in silico* analyses that predicted a similar pattern of ID in NHE1s from a broad array of vertebrate species, these data show that ID is a highly conserved feature of the cytoplasmic domain of NHE1. This is the first time that ID has been experimentally characterized in any carrier protein. The finding that ID is highly conserved in NHE1 in spite of substantial sequence differences agrees well with sequence evolution analyses, suggesting that ID, rather than specific sequence, is the evolutionary constraint for IDPs.[19,20] Very few studies have experimentally correlated ID in evolutionary related proteins, and although conservation of ID has been reported,[21,40] this is to our knowledge the first study in which conservation of ID has been found to correlate with extended similarities in SSP profile (compare e.g. with ref 40).

What is the physiological relevance of ID in NHE1? Recently, the C-terminal tail of the *D. melanogaster* Shaker K^+ channel was shown to be disordered, and the tail was assigned a "fishing rod" function in interaction of the channel with other proteins.[26] This finding is particularly interesting because while these proteins are otherwise fundamentally different and share no sequence homology, the C-terminal tails of the Shaker K^+ channel and NHE1 both act as protein interaction scaffolds.[26,54] Of particular interest in this regard may be that several functionally important NHE1 binding sites overlap,[54] and ID may be a way to facilitate flexible interactions of the same region with multiple partners, similar to the "signaling hub" type of proteins.[55,56] ID is overrepresented in proteins with roles in cellular signaling[16] and predicted to be a general feature of the intracellular domains of membrane-bound proteins.[57,58] Hence, we predict that ID may be a common feature that enables protein−protein interactions in ion transport proteins.

Both the h- and paNHE1*cdt*s contain several potential MoRFs, i.e., regions of transient secondary structure within the ID region, through which IDPs often interact with their binding partners. Most of these overlap in h- and paNHE1, and although amplitudes differed, the overall SSP profiles were surprisingly similar in the *cdt*s from the two species. The high similarity and specific differences parallel the known similarities and differences in regulation of h- and paNHE1. For instance, both homologues

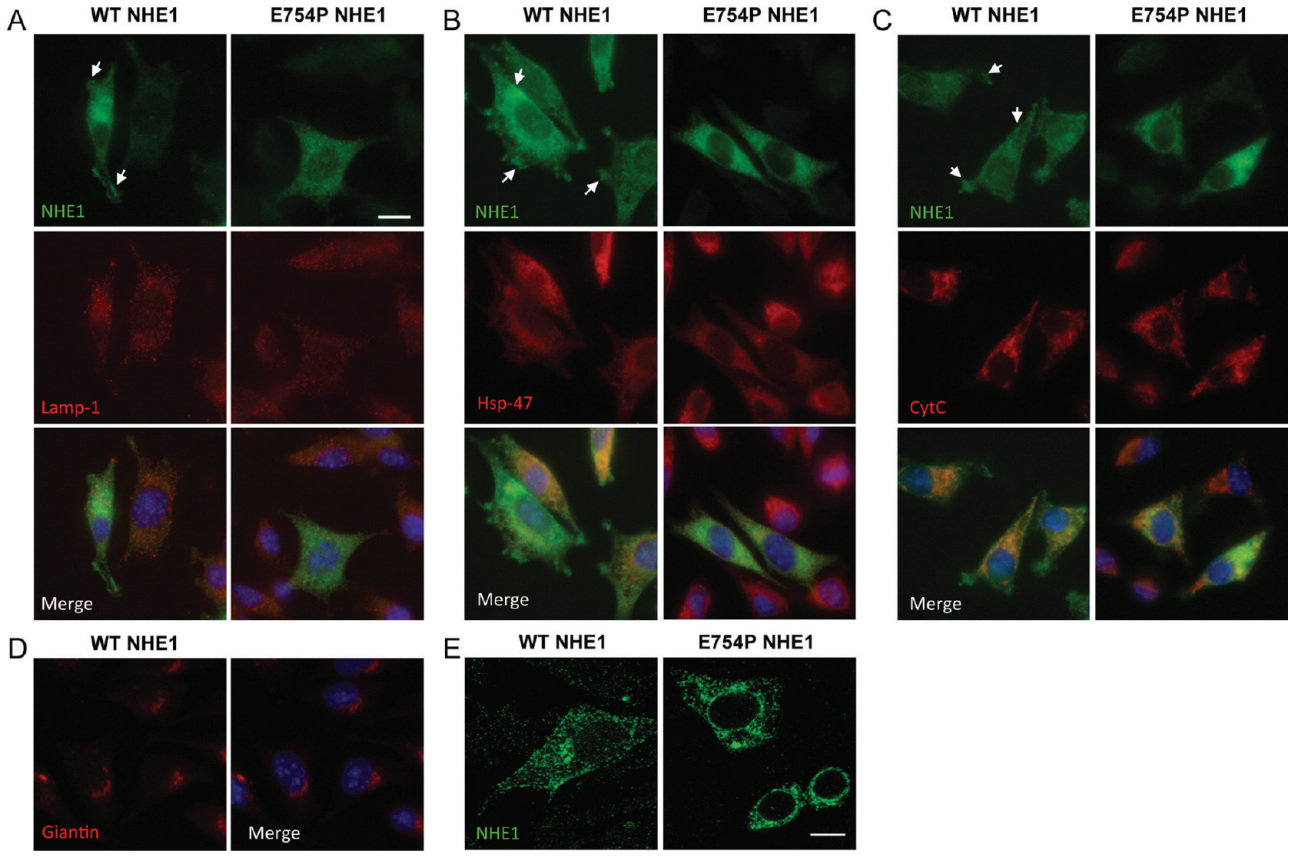

Figure 7. The paNHE1^{E754P} mutation is associated with intracellular accumulation of NHE1. Immunofluorescence analysis of AP1 cells expressing WT and E754 mutant paNHE1. NHE1 was labeled using a polyclonal antibody (green), and nuclei are stained using DAPI. (A) Co-staining with a monoclonal antibody against the lysosome/late endosome marker Lamp 1. (B) Co-staining with a monoclonal antibody against the ER marker Hsp-47. (C) Co-staining with a monoclonal antibody against the mitochondrial marker cytochrome *c*. (D) Staining of WT cells with a monoclonal antibody against the Golgi marker Giantin. The partial localization of WT NHE1 to the plasma membrane is strongly reduced for paNHE1^{E754P}. Instead, paNHE1^{E754P} accumulates intracellularly and most predominantly in a perinuclear region. While there is not complete overlap of paNHE1^{E754P} labeling with any of the organellar markers tested, there is partial colocalization with Hsp-47, suggesting accumulation in the ER. Scale bar: 5 μm. (E) Confocal images of preparations as above, showing in a 1 μm optical section the localization of WT paNHE1 and paNHE1^{E754P}. Scale bar: 10 μm. The images shown are representative of at least three independent experiments per condition.

are activated by low pH_i and osmotic shrinkage, yet only the mammalian NHE1s are activated by Ca^{2+} and growth factors, while paNHE1 and other fish NHE1s are activated by cAMP-PKA signaling.[43,44] Significantly, $H2_h$, which has no parallel in paNHE1, coincides with the proposed ERK phosphorylation sites S766, S770, and S771[59] and could thus play a role as an interaction site regulated by this modification. Likewise, the variance in SSP amplitude may be linked to the different operating temperatures of the two species, but this warrants further investigations.

Little is known regarding the specific intracellular trafficking mechanisms of NHE1. For the mammalian NHE1s, the fully glycosylated form containing N- and O-linked oligosaccharides is expressed at the cell surface, while a lower molecular weight form is present in the ER and only contains N-linked high-mannose oligosaccharide.[52] Disruption of the major MoRF in paNHE1, $H2_{pa}$ (corresponding to $H3_h$ in hNHE1), by the mutation E754P was confirmed by NMR spectroscopy *in vitro*. *In vivo*, this mutation was associated with a marked decrease in NHE1 glycosylation, intracellular retention of NHE1, at least partially in the ER, and decreased NHE1 activity after an acid load. These data strongly indicate that the region including $H2_{pa}/H3_h$ plays a role in allowing NHE1 to exit from the ER and be trafficked to the plasma membrane. These studies also have a broader experimental relevance, since they show that detection of partially folded MoRFs by NMR and their subsequent mutagenic disruption *in vivo* is a promising general strategy for elucidating the functions of ID regions in proteins. ER export has to our knowledge not been directly addressed for carrier proteins; several ion channels have been reported to interact with the COPII vesicle component, Sec24, through di- (or tri-) acidic ER export motifs (D/E-X-D/E) or (D/E-X-D/E-X-D/E).[60,61] Similar di- and triacidic ER export motifs are located in paNHE1*cdt*. One motif that is conserved between h- and paNHE1*cdt* is in paNHE1*cdt* located in the region around the mutation site, (D_{770}-E-E_{772}-E-D_{774}), mirrored in a similar acidic region in hNHE1*cdt* (E_{803}-PG-E_{806}-G-E_{808}) and located C-terminally to $H2_{pa}/H3_h$. Both sites have negative SSP scores. Moreover, the LSD box partially contained within and partially adjacent to the $H2_{pa}/H3_h$ MoRF contains a fully conserved aspartic acid ($D797_h/D764_{pa}$). While additional studies are required to experimentally address this question, it is possible that a similar mechanism may be essential for NHE1 export from the ER and that the E754P mutation interferes with the interaction of NHE1

dx.doi.org/10.1021/bi1019989 |*Biochemistry* 2011, 50, 3469–3480

with Sec24 or with a related protein. Since disruption of the $H2_{pa}$ MoRF leads to ER accumulation, our data also suggest that the ER export motif may be expanded to include a recognition helix in connection with the acidic residues. It may be noted that the LSD box also coincides with a previously proposed binding site for carbonic anhydrase II[11] and with a predicted PKB phosphorylation site (hNHE1-S796[62]); hence, additional functions for this region are very possible.

CONCLUSION

In conclusion, we have demonstrated that NHE1 possesses a large intracellular region of ID. This ID region is evolutionarily conserved in vertebrate NHE1s despite highly divergent sequences, consistent with a conserved functional role. Within this region, several possible MoRFs were identified, which were also largely conserved. When the most prominent of these putative MoRFs was disrupted by introduction of a proline, paNHE1 function was markedly reduced, with reduced plasma membrane localization at least in part reflecting retention of NHE1 in the ER. These studies suggest that the outermost part of the C-terminal tail of NHE1 may be important for recognition by the ER export machinery. Moreover, they identify ID as a novel component in the regulation of the complex protein−protein interactions at the NHE1 C-terminal tail.

ASSOCIATED CONTENT

Supporting Information. Figures S1−S3. This material is available free of charge via the Internet at http://pubs.acs.org.

AUTHOR INFORMATION

Corresponding Author

*Phone +45 35321546, e-mail SFPedersen@bio.ku.dk (S.F.P); phone +45 35322081, fax +45 35322028, e-mail bbk@bio.ku.dk (B.B.K.).

Funding Sources

This work was supported in part by the Danish Research councils (#21040604/FNU to B.B.K., #09-065569/FSS to S.F.P.), The Danish Cancer Society (R2-A273-09-S2/SFP), the Novo Nordisk Foundation (S.F.P.), and by a scholarship from Novo Nordisk A/S (A.B.N.).

ACKNOWLEDGMENT

We thank Signe Sjørup and Anni Bech Nielsen for excellent technical assistance, Mark Musch, University of Chicago, for the kind gift of NHE1 antibody, Sergio Grinstein, University of Toronto, for AP1 cells, and EMBL Hamburg for SAXS assistance.

ABBREVIATIONS

BCECF-AM, 2′,7′-bis(2-carboxyethyl)-5,6-carboxyfluorescein, tetraacetoxymethyl ester; CD, circular dichroism; *cdt*, C-terminal distal tail;; *cpt*, C-terminal proximal tail; *ct*, C-terminal tail; DSS, 4,4-dimethyl-4-silapentane-1-sulfonic acid; DTT, dithiothreitol; FID, free induction decay; HSQC, heteronuclear single quantum coherence; ID, intrinsic disorder; IDP, intrinsically disordered protein; MoRF, molecular recognition feature; NHE1, Na^+/H^+ exchanger 1; h, human; pa, *Pleuronectes americanus*; NMR, nuclear magnetic resonance; SAXS, small-angle X-ray scattering; SSP, secondary structure propensity.

REFERENCES

(1) Pedersen, S. F. (2006) The Na^+/H^+ exchanger NHE1 in stress-induced signal transduction: implications for cell proliferation and cell death. *Pflugers Arch. 452*, 249–259.

(2) Shrode, L. D., Gan, B. S., D'Souza, S. J. A., Orlowski, J., and Grinstein, S. (1998) Topological analysis of NHE1, the ubiquitous Na^+/H^+ exchanger using chymotryptic cleavage. *Am. J. Phys. Cell. Phys. 275*, C431–C439.

(3) Wakabayashi, S., Pang, T. X., Su, X. H., and Shigekawa, M. (2000) A novel topology model of the human Na^+/H^+ exchanger isoform 1. *J. Biol. Chem. 275*, 7942–7949.

(4) Nygaard, E. B., Lagerstedt, J. O., Bjerre, G., Poulsen, K. A., Meinild, S., Rigor, R. R., Pedersen, S. F., Voss, J. C., and Cala, P. M. (2010) Structural modeling and electron paramagnetic resonance spectroscopy of the human Na^+/H^+ Exchanger isoform 1. *J. Biol. Chem.*resubmitted after revision.

(5) Bertrand, B., Wakabayashi, S., Ikeda, T., Pouyssegur, J., and Shigekawa, M. (1994) The Na^+/H^+ exchanger isoform 1 (NHE1) is a novel member of the calmodulin-binding proteins. Identification and characterization of calmodulin-binding sites. *J. Biol. Chem. 269*, 13703–13709.

(6) Ben Ammar, Y., Takeda, S., Hisamitsu, T., Mori, H., and Wakabayashi, S. (2006) Crystal structure of CHP2 complexed with NHE1-cytosolic region and an implication for pH regulation. *EMBO J. 25*, 2315–2325.

(7) Zaun, H. C., Shrier, A., and Orlowski, J. (2008) Calcineurin B homologous protein 3 promotes the Biosynthetic maturation, cell surface stability, and optimal transport of the Na^+/H^+ exchanger NHE1 isoform. *J. Biol. Chem. 283*, 12456–12467.

(8) Mishima, M., Wakabayashi, S., and Kojima, C. (2007) Solution structure of the cytoplasmic region of Na+/H+ exchanger 1 complexed with essential cofactor calcineurin B homologous protein 1. *J. Biol. Chem. 282*, 2741–2751.

(9) Denker, S. P., Huang, D. C., Orlowski, J., Furthmayr, H., and Barber, D. L. (2000) Direct binding of the Na-H exchanger NHE1 to ERM proteins regulates the cortical cytoskeleton and cell shape independently of H^+ translocation. *Mol. Cells 6*, 1425–1436.

(10) Silva, N., Haworth, R. S., Singh, D., and Fliegel, L. (1995) The carboxyl-terminal region of the Na^+/H^+ exchanger interacts with mammalian heat shock protein. *Biochemistry 34*, 10412–10420.

(11) Li, X. J., Liu, Y. S., Alvarez, B. V., Casey, J. R., and Fliegel, L. (2006) A novel carbonic anhydrase II binding site regulates NHE1 activity. *Biochemistry 45*, 2414–2424.

(12) Gebreselassie, D., Rajarathnam, K., and Fliegel, L. (1998) Expression, purification, and characterization of the carboxyl-terminal region of the Na^+/H^+ exchanger. *Biochem. Cell. Biol. 76*, 837–842.

(13) Hisamitsu, T., Pang, T., Shigekawa, M., and Wakabayashi, S. (2004) Dimeric interaction between the cytoplasmic domains of the Na+/H+ exchanger NHE1 revealed by symmetrical intermolecular cross-linking and selective co-immunoprecipitation. *Biochemistry 43*, 11135–11143.

(14) Dunker, A. K., Lawson, J. D., Brown, C. J., Williams, R. M., Romero, P., Oh, J. S., Oldfield, C. J., Campen, A. M., Ratliff, C. R., Hipps, K. W., Ausio, J., Nissen, M. S., Reeves, R., Kang, C. H., Kissinger, C. R., Bailey, R. W., Griswold, M. D., Chiu, M., Garner, E. C., and Obradovic, Z. (2001) Intrinsically disordered protein. *J. Mol. Graphics Modell. 19*, 26–59.

(15) Wright, P. E., and Dyson, H. J. (1999) Intrinsically unstructured proteins: Re-assessing the protein structure-function paradigm. *J. Mol. Biol. 293*, 321–331.

(16) Iakoucheva, L. M., Brown, C. J., Lawson, J. D., Obradovic, Z., and Dunker, A. K. (2002) Intrinsic disorder in cell-signaling and cancer-associated proteins. *J. Mol. Biol. 323*, 573–584.

(17) Danielsson, J., Liljedahl, L., Barany-Wallje, E., Sonderby, P., Kristensen, L. H., Martinez-Yamout, M. A., Dyson, H. J., Wright, P. E., Poulsen, F. M., Maler, L., Graslund, A., and Kragelund, B. B. (2008) The intrinsically disordered RNR inhibitor Sml1 is a dynamic dimer. *Biochemistry 47*, 13428–13437.

(18) Ward, J. J., Sodhi, J. S., McGuffin, L. J., Buxton, B. F., and Jones, D. T. (2004) Prediction and functional analysis of native disorder in proteins from the three kingdoms of life. *J. Mol. Biol. 337*, 635–645.

(19) Brown, C. J., Takayama, S., Campen, A. M., Vise, P., Marshall, T. W., Oldfield, C. J., Williams, C. J., and Dunker, A. K. (2002) Evolutionary rate heterogeneity in proteins with long disordered regions. *J. Mol. Evol. 55*, 104–110.

(20) Denning, D. P., and Rexach, M. F. (2007) Rapid evolution exposes the boundaries of domain structure and function in natively unfolded FG nucleoporins. *Mol. Cell. Proteom. 6*, 272–282.

(21) Daughdrill, G. W., Narayanaswami, P., Gilmore, S. H., Belczyk, A., and Brown, C. J. (2007) Dynamic behavior of an intrinsically unstructured linker domain is conserved in the face of negligible amino acid sequence conservation. *J. Mol. Evol. 65*, 277–288.

(22) Mittag, T., Kay, L. E., and Forman-Kay, J. D. (2010) Protein dynamics and conformational disorder in molecular recognition. *J. Mol. Recognit. 23*, 105–116.

(23) Vacic, V., Oldfield, C. J., Mohan, A., Radivojac, P., Cortese, M. S., Uversky, V. N., and Dunker, A. K. (2007) Characterization of molecular recognition features, MoRFs, and their binding partners. *J. Proteome Res. 6*, 2351–2366.

(24) Uversky, V. N., Oldfield, C. J., and Dunker, A. K. (2008) Intrinsically disordered proteins in human diseases: Introducing the D-2 concept. *Annu. Rev. Biophys. 37*, 215–246.

(25) Garza, A. M., Khan, S. H., and Kumar, R. (2010) Site-specific phosphorylation induces functionally active conformation in the intrinsically disordered N-terminal activation function (AF1) domain of the glucocorticoid receptor. *Mol. Cell. Biol. 30*, 220–230.

(26) Magidovich, E., Orr, I., Fass, D., Abdu, U., and Yifrach, O. (2007) Intrinsic disorder in the C-terminal domain of the Shaker voltage-activated K+ channel modulates its interaction with scaffold proteins. *Proc. Natl. Acad. Sci. U.S.A. 104*, 13022–13027.

(27) Thompson, J. D., Higgins, D. G., and Gibson, T. J. (1994) CLUSTAL W: improving the sensitivity of progressive multiple sequence alignment through sequence weighting, position-specific gap penalties and weight matrix choice. *Nucleic Acids Res. 22*, 4673–4680.

(28) Emanuelsson, O., Brunak, S., von Heijne, G., and Nielsen, H. (2007) Locating proteins in the cell using TargetP, SignalP and related tools. *Nature Protoc. 2*, 953–971.

(29) Pedersen, S. F., King, S. A., Nygaard, E. B., Rigor, R. R., and Cala, P. M. (2007) NHE1 inhibition by amiloride- and benzoylguanidine-type compounds - Inhibitor binding loci deduced from chimeras of NHE1 homologues with endogenous differences in inhibitor sensitivity. *J. Biol. Chem. 282*, 19716–19727.

(30) Rotin, D., and Grinstein, S. (1989) Impaired cell volume regulation in Na+-H+ exchange-deficient mutants. *Am. J. Phys. 257*, C1158–C1165.

(31) Kjaergaard, M., Norholm, A. B., Hendus-Altenburger, R., Pedersen, S. F., Poulsen, F. M., and Kragelund, B. B. (2010) Temperature-dependent structural changes in intrinsically disordered proteins: formation of alpha-helices or loss of polyproline II? *Protein Sci. 19*, 1555–1564.

(32) Ikura, M., Kay, L. E., and Bax, A. (1990) A novel approach for sequential assignment of H-1, C-13, and N-15 spectra of larger proteins —heteronuclear triple-resonance 3-dimensional NMR spectroscopy— Application to calmodulin. *Biochemistry 29*, 4659–4667.

(33) Bax, A., and Ikura, M. (1991) An efficient 3D NMR technique for correlating the proton and 15N backbone amide resonances with the alpha-carbon of the preceding residue in uniformly 15N/13C enriched proteins. *J. Biol. NMR 1*, 99–104.

(34) Wittekind, M., and Mueller, L. (1993) HNCACB, A high-sensitivity 3D. NMR experiment to correlate amide-proton and nitrogen reso- nances with the alpha-carbon and beta-carbon resonances in proteins. *J. Magn. Reson., Ser. B 101*, 201–205.

(35) Grzesiek, S., and Bax, A. (1992) Correlating backbone amide and side chain resonances in larger proteins by multiple relayed triple resonance NMR. *J. Am. Chem. Soc. 114*, 6291–6293.

(36) Clubb, R. T., Thanabal, V., and Wagner, G. (1992) A constant-time 3-dimensional triple-resonance pulse scheme to correlate intraresidue H-1(N), N-15, and C-13(′) chemical shifts in N-15-C-13-labeled proteins. *J. Magn. Reson. 97*, 213–217.

(37) Delaglio, F., Grzesiek, S., Vuister, G. W., Zhu, G., Pfeifer, J., and Bax, A. (1995) NMRPIPE - A MULTIDIMENSIONAL SPECTRAL PROCESSING SYSTEM BASED ON UNIX PIPES. *J. Biol. NMR 6*, 277–293.

(38) Vranken, W. F., Boucher, W., Stevens, T. J., Fogh, R. H., Pajon, A., Llinas, P., Ulrich, E. L., Markley, J. L., Ionides, J., and Laue, E. D. (2005) The CCPN data model for NMR spectroscopy: Development of a software pipeline. *Proteins: Struct., Funct., Bioinf. 59*, 687–696.

(39) Zimmerman, D. E., Kulikowski, C. A., Huang, Y. P., Feng, W. Q., Tashiro, M., Shimotakahara, S., Chien, C. Y., Powers, R., and Montelione, G. T. (1997) Automated analysis of protein NMR assignments using methods from artificial intelligence. *J. Mol. Biol. 269*, 592–610.

(40) Marsh, J. A., Singh, V. K., Jia, Z. C., and Forman-Kay, J. D. (2006) Sensitivity of secondary structure propensities to sequence differences between alpha- and gamma-synuclein: Implications for fibrillation. *Protein Sci. 15*, 2795–2804.

(41) Wishart, D. S., Bigam, C. G., Yao, J., Abildgaard, F., Dyson, H. J., Oldfield, E., Markley, J. L., and Sykes, B. D. (1995) H-1, C-13 and N-15 Chemical-Shift Referencing in Biomolecular NMR. *J. Biomol. NMR 6*, 135–140.

(42) Pedersen, S. F., and Cala, P. M. (2004) Comparative biology of the ubiquitous Na+/H+ exchanger, NHE1: Lessons from erythrocytes. *J. Exp. Zool., Part A 301A*, 569–578.

(43) Pedersen, S. F., King, S. A., Rigor, R. R., Zhuang, Z. P., Warren, J. M., and Cala, P. M. (2003) Molecular cloning of NHE1 from winter flounder RBCs: activation by osmotic shrinkage, cAMP, and calyculin A. *Am. J. Phys. Cell. Phys. 284*, C1561–C1576.

(44) Holt, M. E. V., King, S. A., Cala, P. M., and Pedersen, S. F. (2006) Regulation of the Pleuronectes americanus Na+/H+ exchanger by osmotic shrinkage, beta-adrenergic stimuli, and inhibition of Ser/Thr protein Phosphatases. *Cell: Biochem. Biophys. 45*, 1–18.

(45) Tompa, P. (2002) Intrinsically unstructured proteins. *Trends Biochem. Sci. 27*, 527–533.

(46) Uversky, V. N. (2002) Cracking the folding code. Why do some proteins adopt partially folded conformations, whereas other don't? *FEBS Lett. 514*, 181–183.

(47) Receveur-Brechot, V., Bourhis, J. M., Uversky, V. N., Canard, B., and Longhi, S. (2006) Assessing protein disorder and induced folding. *Proteins: Struct., Funct., Bioinf. 62*, 24–45.

(48) Kalthoff, C. (2003) A novel strategy for the purification of recombinantly expressed unstructured protein domains. *J. Chromatogr., B: Anal. Technol. Biomed. Life Sci. 786*, 247–254.

(49) Uversky, V. N. (2002) What does it mean to be natively unfolded? *Eur. J. Biochem. 269*, 2–12.

(50) Reddy, T., and Rainey, J. K. (2010) Interpretation of biomolecular NMR spin relaxation parameters. *Biochem. Cell. Biol. 88*, 131–142.

(51) Munoz, V., and Serrano, L. (1994) Elucidating the folding problem of helical peptides using empirical parameters. *Nat. Struct. Biol. 1*, 399–409.

(52) Counillon, L., Pouyssegur, J., and Reithmeier, R. A. F. (1994) The Na^+/H^+ exchanger NHE1 possesses N- and O-linked glycosylation restricted to the first N-terminal extracellular domain. *Biochemistry 33*, 10463–10469.

(53) Schneider, L., Stock, C. M., Dieterich, P., Jensen, B. H., Pedersen, L. B., Satir, P., Schwab, A., Christensen, S. T., and Pedersen, S. F. (2009) The Na+/H+ exchanger NHE1 is required for directional migration stimulated via PDGFR-alpha in the primary cilium. *J. Cell Biol. 185*, 163–176.

(54) Meima, M. E., Mackley, J. R., and Barber, D. L. (2007) Beyond ion translocation: structural functions of the sodium-hydrogen exchanger isoform-1. *Curr. Opin. Nephrol. Hypertens. 16*, 365–372.

(55) Kim, P. M., Sboner, A., Xia, Y., and Gerstein, M. (2008) The role of disorder in interaction networks: a structural analysis. *Mol. Syst. Biol. 4*, 179.

(56) Dunker, A. K., Cortese, M. S., Romero, P., Iakoucheva, L. M., and Uversky, V. N. (2005) Flexible nets. The roles of intrinsic disorder in protein interaction networks. *FEBS J. 272*, 5129–5148.

(57) Minezaki, Y., Homma, K., and Nishikawa, K. (2007) Intrinsically disordered regions of human plasma membrane proteins preferentially occur in the cytoplasmic segment. *J. Mol. Biol. 368*, 902–913.

(58) Xue, B., Li, L. W., Meroueh, S. O., Uversky, V. N., and Dunker, A. K. (2009) Analysis of structured and intrinsically disordered regions of transmembrane proteins. *Mol. Biosyst. 5*, 1688–1702.

(59) Coccaro, E., Karki, P., Cojocaru, C., and Fliegel, L. (2009) Phenylephrine and sustained acidosis activate the neonatal rat cardiomyocyte Na+/H+ exchanger through phosphorylation of amino acids Ser(770) and Ser(771). *Am. J. Phys.: Heart Circ. 297*, H846–H858.

(60) Sieben, C., Mikosch, M., Brandizzi, F., and Homann, U. (2008) Interaction of the K+-channel KAT1 with the coat protein complex II coat component Sec24 depends on a di-acidic endoplasmic reticulum export motif. *Plant J. 56*, 997–1006.

(61) Mikosch, M., and Homann, U. (2009) How do ER export motifs work on ion channel trafficking? *Curr. Opin. Plant Biol. 12*, 685–689.

(62) Snabaitis, A. K., Cuello, F., and Avkiran, M. (2008) Protein kinase B/Akt phosphorylates and inhibits the cardiac Na^+/H^+ exchanger NHE1. *Circ. Res. 103*, 881–U256.